

Resource allocation for Millimeter Wave mMIMO-NOMA System with IRS

Bing Ning^{1*}, Shuang Li¹, Xinli Wu², and Wanming Hao²

¹School of Electronic and Information Engineering, Zhongyuan University of Technology,
Zhengzhou, 450007-China

²School of Information Engineering, Zhengzhou University,
Zhengzhou, 450001-China

[E-mail: bingning0106@zut.edu.cn]

*Corresponding author: Wanming Hao

*Received February 14, 2024; revised June 5, 2024; accepted June 24, 2024;
published July 31, 2024*

Abstract

In order to improve the coverage and achieve massive spectrum access, non-orthogonal multiple access (NOMA) technology is applied in millimeter wave massive multiple-input multiple-output (mMIMO) communication network. However, the power assumption of active sensors greatly limits its wide applications. Recently, Intelligent Reconfigurable Surface (IRS) technology has received wide attention due to its ability to reduce power consumption and achieve passive transmission. In this paper, spectral efficiency maximum problem in the millimeter wave mMIMO-NOMA system with IRS is considered. The sparse RF chain antenna structure is designed at the base station based on continuous phase modulation. Furthermore, a joint optimization problem for power allocation, power splitting, analog precoding and IRS reconfigurable matrices are constructed, which aim to achieve the maximum spectral efficiency of the system under the constraints of user's quality of service, minimum energy harvesting and total transmit power. A three-stage iterative algorithm is proposed to solve the above mentioned non-convex optimization problems. We obtain the local optimal solution by fixing some optimization parameters firstly, then introduce the relaxation variables to realize the global optimal solution. Simulation results show that the spectral efficiency of the proposed scheme is superior compared to the conventional system with phase shifter modulation. It is also demonstrated that IRS can effectively assist mmWave communication and improve the system spectral efficiency.

Keywords: IRS, mmWave-mMIMO, NOMA, resource allocation, convex optimization

1. Introduction

Millimeter-wave mMIMO system [1] is widely applied in the wireless communication due to the advantages of improving spectrum utilization. To achieve massive access, large-scale antennas at base station are deployed to form high-gain directional beams. This could result in a large amount of power consumption and causing interference between different users. NOMA technology [2] can allow users to share resources non-orthogonally in the same frequency band, and enable multiplexing between multiple users by differentiating on the power and coding scheme of the signals, which effectively solve the problem of spectrum congestion caused by massive user access, and improve the quality of coverage for the edge users. Therefore, NOMA technology is introduced in the millimeter-wave mMIMO system, that can increase the number of users and reduce the cost of the radio frequency (RF) chains.

Spectral efficiency is a central issue in the millimeter wave mMIMO-NOMA system as it is directly related the number of access users within a given bandwidth. There are many studies on resource allocation and performance analysis in the millimeter wave mMIMO-NOMA system. For example, the authors in [3] proposed an angular information-based NOMA scheme that significantly improves the total throughput of millimeter-wave MU-MIMO systems by reducing spatial interference and optimizing user sequencing and power allocation. The resource allocation by jointly optimizing the corresponding parameters was investigated in [4], [5]. In order to enhance the signal coverage and transmission quality, especially in the case of long distances between users and BS or high signal attenuation, relay-assisted transmission protocols are used in [6]-[8]. Outage performance was studied to reduce the probability of downtime through amplify-and-forward relaying techniques in [9]. In [10], the power allocation optimization strategy was proposed for maximizing throughput. In [11], the incomplete successive interference cancellation (SIC) was considered, and the optimal power allocation algorithm is derived to minimize the outage probability. Different analysis of energy efficiency from multiple perspectives have been investigated by the following papers, respectively. In [12], game theory was used to design the pricing mechanism and the resource allocation strategy for the maximum energy efficiency was studied. The Lagrangian pairwise decomposition method was employed to solve the non-convex optimization problem of resource allocation strategy in [13], [14], with the difference that the former focuses on the resource allocation for nonlinear energy models, while the latter focuses on the energy efficiency of uplink NOMA systems. In order to somehow improve the reliability of the communication system with the reduction of the system overhead, [15] investigated resource allocation for beamforming and power, which resulted in a lower outage probability of the system. The eavesdropper was introduced in [16] to study the security energy efficiency under several different antenna structures for mmWave-NOMA system. The authors in [17] and [18] adopted the user grouping and cluster formation strategies to optimize the resource allocation (such as channel correlation, gain differences, power, etc.), respectively. This strategy helped to better utilize the advantages of NOMA technology to improve energy efficiency and throughput in the millimeter wave mMIMO system.

However, there are still some technical bottlenecks in the above researches, for example, abnormal communication between base station and users may be produced due to the poor penetrability, short propagation distance and susceptibility to interference of the millimeter wave, and performance degradation and power consumption increases in non-ideal channel condition are caused by the complex active devices. Intelligent Reconfigurable Surface communication technology can enhance the signal transmission quality and coverage by

adjusting the phase and amplitude of the reflective elements to improve the performance of the network and significantly reduce power consumption. In [19], The precoding matrix was designed to enhance the millimeter wave coverage in the IRS-assisted millimeter-wave system and the jointly optimal problem of the phase shift matrix and precoding matrix was investigated to maximize the throughput. In order to improve coverage and save power consumption, the authors in [20] focused on the MIMO-NOMA system with IRS and intergroup and clustering methods were proposed in order to reduce the total system transmit power. Furthermore, power consumption is minimized by simultaneously optimizing beamforming and phase shifting. Due to the high propagation loss of millimeter waves, it is difficult to communicate over long distances. Therefore, the authors in [21] proposed an adaptive resource allocation scheme in a dual-user millimeter wave NOMA system with IRS to optimize the resource allocation.

Recently, simultaneous wireless power and data transfer (SWIPT) have received greatly attention, which can provide energy for the receiving device while sending information [22]. The SWIPT technology can reduce the energy waste and improve the efficiency of energy utilization. Thus, some studies have applied the SWIPT technology to IRS-assisted mmWave-MIMO-NOMA system to reduce power consumption. In [23], the phase modulation array-based hybrid precoding matrix was designed and a cluster head selection algorithm was proposed to optimize the resource allocation. Compared to [23], the works in [24] introduced the SWIPT technology to the mMIMO-NOMA system to realize passive transmission and the power allocation strategy was proposed to maximize energy efficiency. To solve the non-convex problem, the outer and inner layers based on the Dinkelbach's method was investigated. In [25], two types of IRS-assisted antenna arrays were designed to maximize the mutual information and obtained the approximate optimal precoding matrix. In [26], hybrid precoding was designed by using the active and passive hardware to enhance the data transmission and the jointly optimal algorithm for BS's precoding matrix and IRS's phase shift parameters was proposed. The works in [27] also studied the resource allocation in the IRS-assisted mmWave-MIMO-NOMA system with SWIPT, but the authors in [27] further considered the influence of the non-ideal conditions on the system performance. In [28], the cluster-head selection algorithm was proposed in the SWIPT-based MIMO-NOMA system to pair the beamform with the associated user. The authors of [29] considered the actual SWIPT-based mMIMO system application scenarios such as the imperfect RF signal response, low sensitivity of hardware components. Furthermore, the hybrid precoding scheme based on the non-ideal parameters was designed to maximize the throughput. In [30], the jointly optimizing algorithm for the transmission power and power splitting parameter was proposed to achieve the maximum spectrum and energy efficiency.

Most of the existing works have made a lot of contribution in the precoding scheme, the performance analysis and the optimal resource allocation strategy for the millimeter wave mMIMO system or the millimeter wave mMIMO- NOMA system with IRS. However, the high-resolution low-power characteristics in continuous phase modulation networks require the BS to adopt the corresponding analog precoding for continuous phase modulation network design. Therefore, there still exists some challenges in the millimeter wave mMIMO-NOMA system with IRS. First, the analog precoding design based on phase shifters with high resolution and high energy requirement results in large energy consumption, that lead to a large amount of energy consumption in the massive access mode. From the perspective of future energy strategy, it is important to introduce the passive transmission mode to realize the optimal resource allocation. Second, the non-convex problems formed in resource allocation strategies are challenging. It is necessary to solve such problems efficiently with fast

converging and low complexity algorithms. When solving complex problems involving coupled optimization variables, the importance of using corresponding algorithms cannot be ignored. Thus, how to achieve the optimal resource allocation to maximize the spectral efficiency is an urgent problem at present.

To address the above problems, this paper constructs a millimeter wave mMIMO-NOMA system based on IRS to realize passive transmission. In this system, the resource allocation strategy is studied to maximize the throughput by jointly optimizing the parameters such as power allocation factor, power splitting factor, beamforming vectors, and IRS reflection matrix. The specific contributions are as follows:

1) The millimeter wave mMIMO-NOMA system based on IRS is constructed to realize passive transmission and multi-user grouping. The impact of the large-scale antenna structure on the system performance is further considered. Thus, the sparse RF chain antenna structure based on continuous phase modulation is proposed to save the energy consumption. The successive interference cancellation is also used to reduce the interference between users in the same group. On this basis, the resource allocation optimization strategy is studied to maximize the throughput by jointly optimize the power allocation, power splitting factor, analog precoding vector, and IRS reflection matrix under the corresponding constraint, such as the beamforming constraint, energy harvest constraint, etc.

2) The theoretical analysis shows that the above optimization problem is a non-convex optimization problem. In order to find the optimal solution, a three-stage joint optimization algorithm based on Successive convex approximation (SCA) and Alternating optimization (AO) methods is proposed. In the first stage, the optimal power allocation factor and power splitting factor are obtained by introducing the auxiliary variables to the optimization problem with the other given parameters. In the second stage, the analog beam vector for the fixed IRS reflection matrix is designed by the non-convex optimization transformation algorithm based on the optimal solution in the first stage. In the third stage, the non-convex optimal resource allocation for the IRS reflection matrix is transformed into convex optimization problem by using the SCA method based on the above stages.

3) The numerical results show that the spectral efficiency increases with the increase of the total transmitted power. In addition, the number of IRS reflective elements and transmitting antennas are the important factors that affect the spectral efficiency of the proposed system. Furthermore, it is demonstrated that the spectral efficiency of the system with continuous phase shift is close to that of system with discrete phase shift when the quantization bit is large enough.

A. Notations

$\text{Conj}(\cdot)$ and $(\cdot)^H$ denote the conjugate and the transpose operations, respectively. $|\cdot|$ and $\|\cdot\|$ denotes the absolute value and the Euclidean norm of a vector. $\text{Diag}\{\cdot\}$ denotes a vector that consists of the diagonal elements of a matrix or a diagonal matrix where the diagonal elements are from a vector. $\mathbb{C}^{M \times N}$ means the space of $M \times N$ complex matrix.

2. System Model and Problem Formulation

A. System Model

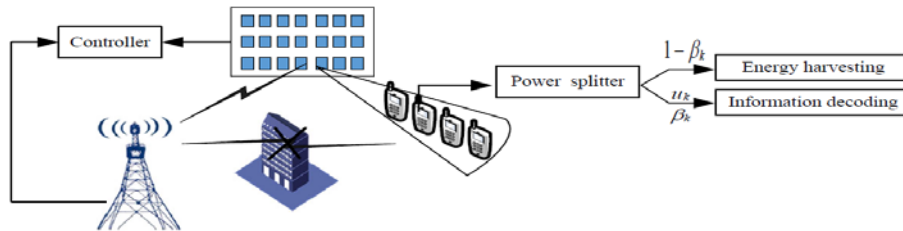


Fig. 1. IRS system model.

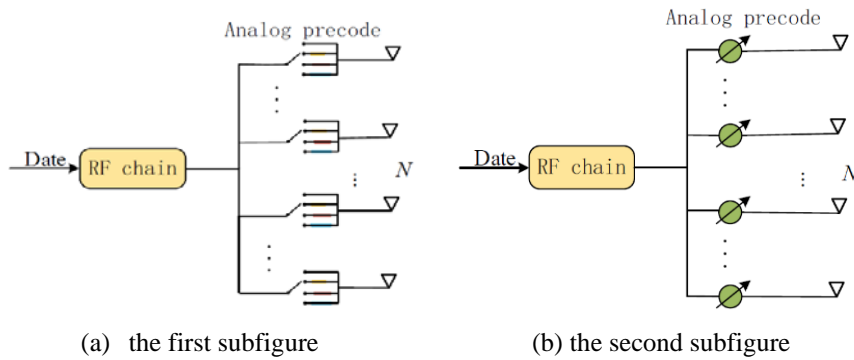


Fig. 2. The sparse RF chain structure at the base station.

The IRS-enabled mmWave-mMIMO-NOMA communication system is shown in Fig. 1, and the sparse RF chain structure of the base station (BS) is shown in Fig. 2. The BS consists of an N_{TX} transmit antenna and an RF chain, and it is assumed that the obstruction of the building makes it impossible for the BS and the user to communicate directly, and the user can only receive the reflected signals with the help of the IRS, in which N_{IRS} and K represent the number of IRS elements and users, respectively.

Considering that the hardware cost and the estimation error due to non-ideal the channel state information (CSI) could be ignored, the IRS phase shift can only be selected from a limited set of discrete values, and the set of discrete phase shift values for each component is as follows:

$$\vartheta_j = \left\{ \frac{2\pi n}{2^B}, n = 0, 1, \dots, 2^B - 1 \right\}, j \in \{1, 2, \dots, N_{IRS}\}, \tag{1}$$

where B represents the resolution of the IRS discrete phase and the calculation of the resource allocation is performed at the BS. The specific process is that the base station transmits the IRS reflection matrix to the controller via a dedicated radio control link, and the connected intelligent controller controls the IRS phase shift and passes the result of the resource allocation (the reflection matrix of the IRS) to the IRS. Then, the signal received by user k is given by:

$$y_k = h_k \Phi G w \sum_{j=1}^K \sqrt{p_j} s_j + n_k, \tag{2}$$

where s_j and p_j represent the signal and power emitted by the base station for the user k , respectively, n_k denotes a Gaussian white noise with mean 0 and variance σ_v^2 , $w \in \mathbb{C}^{N_{\text{TX}} \times 1}$ denotes the analog precoding vector, $G \in \mathbb{C}^{N_{\text{IRS}} \times N_{\text{TS}}}$ denotes the link matrix from the base station to the IRS, $\Phi = \text{diag}(\lambda_1 e^{j\theta_1}, \dots, \lambda_{N_{\text{IRS}}} e^{j\theta_{N_{\text{IRS}}}}) \in \mathbb{C}^{N_{\text{IRS}} \times N_{\text{IRS}}}$ represents the IRS reflection matrix, where $\lambda_{N_{\text{IRS}}} \in [0, 1]$, denotes the amplitude value of each reflection cell, and $h_k \in \mathbb{C}^{1 \times N_{\text{IRS}}}$ represents the channel vector from the IRS to the user k .

Given that each user is equipped with a power divider, the signal received from the user is divided into two parts: EH and ID. β_k ($0 < \beta_k < 1$) represents the power splitting factor of the user k , the corresponding energy harvesting signal for user k is as follows:

$$y_k^{\text{EH}} = \sqrt{1 - \beta_k} y_k. \quad (3)$$

Thus, the energy collected by user k is

$$P_k^{\text{EH}} = \eta(1 - \beta_k) (\|h_k \Phi G w\|_2^2 \sum_{j=1}^K p_j + \sigma_v^2), \quad (4)$$

where η denotes the energy conversion factor, $0 < \eta < 1$. Then the signal received for message decoding at the k th user is as follows:

$$y_k^{\text{ID}} = \sqrt{\beta_k} y_k + u_k, \quad (5)$$

where u_k is the noise interference introduced by the power splitter in the process of signal decoding, and its distribution obeys $CN(0, \sigma_u^2)$.

It can be seen that user k is subject to interference from other users, so it is necessary to use the SIC technique at the receiving end to eliminate interference from users with poor channel conditions to users with good channel conditions. Here, the effective channel is $h_k \Phi G w$, that is, the channel gain, the analog precoding, and the IRS reflection matrix jointly determine the effective channel gain of the user. Since the analog precoding and IRS reflection matrices are unknown quantities, a simplified equivalent channel $h_k G$ is used as the judgment condition for the decoding order. Without prejudice to the loss of generality, it is assumed that the user channels are arranged in descending order of the simplified effective channels, i.e.

$$\|h_1 G\|_2 \geq \|h_2 G\|_2 \geq \dots \geq \|h_K G\|_2. \quad (6)$$

From the NOMA protocol, the remaining signal received for ID at the k th user is as follows:

$$\bar{y}_k^{\text{ID}} = \sqrt{\beta_k} \left(h_k \Phi G w \sqrt{p_k} s_k + h_k \Phi G w \sum_{j=1}^{k-1} \sqrt{p_j} s_j + n_k \right) + u_k. \quad (7)$$

B. Problem Formulation

According to equation (7), the signal-to-noise ratio (SINR) of user k can be obtained as follows:

$$\text{SINR}_k = \frac{\|h_k \Phi G w\|_2^2 p_k}{\|h_k \Phi G w\|_2^2 \sum_{j=1}^{k-1} p_j + \sigma_v^2 + \frac{\sigma_u^2}{\beta_k}} \quad (8)$$

From equation (8), the reachable rate of user k and the total rate of the system are obtained as follows:

$$R_k = \log_2(1 + \text{SINR}_k) \quad (9a)$$

$$R_{\text{sum}} = \sum_{k=1}^K R_k \quad (9b)$$

Consequently, the problem of maximizing the spectral efficiency composition of the system can be expressed as follows:

$$\max_{p_k, \beta_k, \Phi, w} R_{\text{sum}} \quad (10a)$$

$$s. t. \sum_{k=1}^K p_k = P_{\text{max}} \quad (10b)$$

$$R_k \geq R_k^{\text{min}}, \forall k \quad (10c)$$

$$P_k^{\text{EH}} \geq P_k^{\text{min}}, \forall k \quad (10d)$$

$$\|w\|_2 \leq 1 \quad (10e)$$

$$|\lambda_j| \leq 1, j \in \{1, 2, \dots, N_{\text{IRS}}\} \quad (10f)$$

$$w_i \in \Gamma, i \in \{1, 2, \dots, N_{\text{TX}}\} \quad (10g)$$

$$\vartheta_j \in \Omega, j \in \{1, 2, \dots, N_{\text{IRS}}\} \quad (10h)$$

where (10b) denotes the constraint on the total transmit power of the base station, (10c) denotes the user QoS constraint, (10d) denotes the user collection energy QoS constraint, (10e) denotes the power constraint for analog precoding, (10f) denotes the modal value constraint for each reflective cell, (10g) denotes the feasible domain constraint for the analog precoding, (10h) denotes the phase shift constraint of each reflection cell. The above objective functions are jointly optimized reflection matrix, analog precoding vector, power allocation, and power splitting. Since the optimization variables are coupled, because of the complexity and specificity of problem (10), it may be difficult to address it directly.

3. Solution of Sum-rate Optimization Problem

To deal with the previously mentioned nonconvex optimization problem, a joint alternating iterative optimization algorithm is proposed to solve problem (10). The original problem (10) is decomposed into three subproblems to be solved separately. In detail, firstly, given the IRS reflection matrix Φ and the analog precoding vector w , the power allocation p_k and power splitting β_k are solved. Secondly, fixing the power allocation p_k , power splitting β_k and IRS reflection matrix Φ , the analog precoding vector w is solved. Finally, solve the IRS reflection matrix Φ based on the obtained power allocation p_k , power splitting β_k , and the analog precoding vector w . Repeat the same operations as above until the problem reaches a state of convergence.

A. Optimization of p_k and β_k Under Fixed Φ and w

In this subsection, given the IRS reflection matrix Φ and the analog precoding vector w , the power allocation p_k and power splitting β_k are then solved. Transforming the original problem (10) gives the following result:

$$\max_{p_k, \beta_k} \sum_{k=1}^K \log_2 \left(1 + \frac{\|h_k \Phi G w\|_2^2 p_k}{\|h_k \Phi G w\|_2^2 \sum_{j=1}^{k-1} p_j + \sigma_v^2 + \frac{\sigma_u^2}{\beta_k}} \right) \quad (11a)$$

$$\text{s. t. (10b), (10c), (10d)} \quad (11b)$$

Since the optimization variables exist in both numerator and denominator, the optimization problem (11) is non-convex. In order to deal with this issue, auxiliary variables τ_k and t_k are first introduced, and the above issues are transformed into as follow:

$$\max_{p_k, \beta_k} \sum_{k=1}^K \log_2(1 + t_k) \quad (12a)$$

$$\text{s. t. (10b), (10c), (10d)} \quad (12b)$$

$$\frac{\|h_k \Phi G w\|_2^2 p_k}{\|h_k \Phi G w\|_2^2 \sum_{j=1}^{k-1} p_j + \sigma_v^2 + \tau_k \sigma_u^2} \geq t_k \quad (12c)$$

$$\tau_k \geq \frac{1}{\beta_k} \quad (12d)$$

Clearly, constraints (10c), (10d), (12c), and (12d) are non-convex. According to the user reachable rate expression (9a), the user QoS constraint (10c) can be transformed into a convex constraint as follows:

$$\|h_k \Phi G w\|_2^2 p_k - \gamma_k \|h_k \Phi G w\|_2^2 \sum_{j=1}^{k-1} p_j - \gamma_k \tau_k \sigma_u^2 \geq \gamma_k \sigma_v^2, \quad (13)$$

where $\gamma_k = 2^{R_k^{\min}} - 1$. Since the power allocation p_k and the power allocation β_k are coupled to each other, the energy acquisition QoS constraint (10d) is challenging to deal with directly.

Therefore, an auxiliary variable \mathfrak{S}_k is introduced. According to Equation (4), (10d) can be decoupled into the following form:

$$\|h_k \Phi G w\|_2^2 \sum_{j=1}^K p_j + \sigma_v^2 \geq \mathfrak{S}_k, \forall k \quad (14a)$$

$$\mathfrak{S}_k \geq \frac{P_k^{\min}}{\eta(1 - \beta_k)} \quad (14b)$$

It's evident that it is linearly convex constrained, while (14b) is nonconvex. According to Schur's supplementary theorem, (14b) can be transformed into matrix form as follows:

$$\begin{bmatrix} \mathfrak{S}_k & \sqrt{\frac{P_k^{\min}}{\eta}} \\ \sqrt{\frac{P_k^{\min}}{\eta}} & (1 - \beta_k) \end{bmatrix} \geq 0 \quad (15)$$

The constraint (12c) has optimization variables in both numerator and denominator, for which the auxiliary variable b_k is introduced, which is transformed into the following form:

$$\| h_k \Phi \text{Gw} \|_2^2 p_k \geq t_k b_k \quad (16a)$$

$$\| h_k \Phi \text{Gw} \|_2^2 \sum_{j=1}^{k-1} p_j + \sigma_v^2 + \tau_k \sigma_u^2 \leq b_k \quad (16b)$$

The two variables on the right-hand side of equation (16a) are coupled together, so it is non-convex. Then we define two functions $f(t_k, b_k)$ and $\tilde{f}(t_k^{(n)}, b_k^{(n)}, t_k^2, b_k^2)$ as follows:

$$f(t_k, b_k) = t_k b_k \quad (17a)$$

$$\tilde{f}(t_k^{(n)}, b_k^{(n)}, t_k^2, b_k^2) = \frac{t_k^{(n)}}{2b_k^{(n)}} b_k^2 + \frac{b_k^{(n)}}{2t_k^{(n)}} t_k^2 \quad (17b)$$

Before further solving the problem, the following theorem is given.

Theorem 1: $\tilde{f}(t_k^{(n)}, b_k^{(n)}, t_k^2, b_k^2) \geq f(t_k, b_k)$ is constraint. Where $t_k^{(n)}$ and $b_k^{(n)}$ are the values of t_k and b_k at the n th iteration.

Proof: It can be obtained from equations (17a) and (17b)

$$\begin{aligned} & \tilde{f}(t_k^{(n)}, b_k^{(n)}, t_k^2, b_k^2) - f(t_k, b_k) \\ &= \frac{t_k^{(n)}}{2b_k^{(n)}} b_k^2 + \frac{b_k^{(n)}}{2t_k^{(n)}} t_k^2 - t_k b_k \\ &= \frac{t_k^{(n)}}{2b_k^{(n)}} \left(b_k^2 + \left(\frac{b_k^{(n)}}{t_k^{(n)}} \right)^2 t_k^2 - \frac{2b_k^{(n)}}{t_k^{(n)}} t_k b_k \right) \\ &= \frac{t_k^{(n)}}{2b_k^{(n)}} \left(b_k - \frac{b_k^{(n)}}{t_k^{(n)}} t_k \right)^2 \geq 0 \end{aligned} \quad (18)$$

According to theorem 1, (19) is constant.

$$\frac{t_k^{(n)}}{2b_k^{(n)}} b_k^2 + \frac{b_k^{(n)}}{2t_k^{(n)}} t_k^2 \geq t_k b_k. \quad (19)$$

Based on this (16a) can be transformed into a convex constraint as follows

$$\| h_k \Phi \text{Gw} \|_2^2 p_k \geq \frac{t_k^{(n)}}{2b_k^{(n)}} b_k^2 + \frac{b_k^{(n)}}{2t_k^{(n)}} t_k^2. \quad (20)$$

It can be found that the constraint conditions (12d) and (14b) are similar. Similarly, Schur's complementary theorem transforms it into the following form.

$$\begin{bmatrix} \tau_k & 1 \\ 1 & \beta_k \end{bmatrix} \geq 0 \quad (21)$$

Finally, question (11) was reformulated as follows:

$$\max_{p_k, \beta_k, t_k, b_k, k=1}^K \sum_{k=1}^K \log_2(1+t_k) \quad (22a)$$

$$\text{s. t. (10b), (13), (14a), (14c), (16), (20), (21)} \quad (22b)$$

Here, Obviously, problem (22) is defined as a convex optimization problem, which can be handled with the help of the convex optimization tool CVX. Summarily, to obtain power allocation p_k and power splitting β_k , alternate iterative solutions are required to solve (22). Specifically, the auxiliary variables $t_k^{(0)}$ and $b_k^{(0)}$ are initialized first, and then problem (22) is solved to obtain $t_k^{(r)}$, $b_k^{(r)}$, $\beta_k^{(r)}$ and $p_k^{(r)}$ of the r th iteration. Next, $t_k^{(0)}$ and $b_k^{(0)}$ are updated with the obtained $t_k^{(r)}$ and $b_k^{(r)}$, and the problem (22) is resolved. Repeat the same steps until the results converge or the number of iterations is maximized. Based on the above derivation, Algorithm 1 proposes the AO-based power allocation and power splitting optimization algorithm.

Algorithm 1: AO-based power allocation and power splitting optimization algorithm

- 1) Parameter settings: fix the reflection matrix $\Phi^{(0)}$ and analog precoding vector $w^{(0)}$, initialize the auxiliary variables $\{t_k^{(0)}, b_k^{(0)}\}$, the number of iterations $r = 1$, and the maximum number of iterations is r_{max} ;
 - 2) for $r = 1: r_{max}$
 - 3) For the given $\{t_k^{(0)}, b_k^{(0)}\}$ and $\{\Phi^{(0)}, w^{(0)}\}$, solve according to Eq. (22) to obtain and $t_k^{(r)}, b_k^{(r)}$
 - 4) Based on obtaining $t_k^{(r)}$ and $b_k^{(r)}$ updating $t_k^{(0)}$ and $b_k^{(0)}$
 - 5) If $t_k^{(r)}$ converges, jump out of the loop and output directly;
 - 6) Otherwise continue to iterate until the for loop ends
 - 7) Output: optimal objective values p_k^* and β_k^*
-

B. Optimization of w Under Fixed Φ, p_k and β_k

In this section, given power allocation p_k , power splitting β_k and IRS reflection matrices Φ , we then optimize analog precoding vector w . The original question (10) is transformed to

$$\max_w \sum_{k=1}^K \log_2 \left(1 + \frac{\|\hat{h}_k w\|_2^2 p_k}{\|\hat{h}_k w\|_2^2 \sum_{j=1}^{k-1} p_j + \sigma_v^2 + \frac{\sigma_u^2}{\beta_k}} \right) \quad (23a)$$

$$\text{s. t. (10c), (10d), (10e), (10g)} \quad (23b)$$

where $\hat{h}_k = h_k \Phi G$. Similarly, to solve problem (23), we introduce the auxiliary variable t'_k and b'_k , and problem (23) can be transformed as follows:

$$\max_w \sum_{k=1}^K \log_2 (1 + t'_k) \tag{24a}$$

$$s. t. \|\hat{h}_k w\|_2^2 p_k \geq t'_k b'_k \tag{24b}$$

$$\|\hat{h}_k w\|_2^2 \sum_{j=1}^{k-1} p_j + \sigma_v^2 + \frac{\sigma_u^2}{\beta_k} \leq b'_k \tag{24c}$$

$$s. t. (10c), (10d), (10e), (10g) \tag{24d}$$

The problem (24) is non-convex. We first use first-order Taylor expansion to approximate the constraint condition (24b) as a linear function. The first-order Taylor series at point \bar{w} on the left side of the equation (24b) is as follows:

$$\|\hat{h}_k w\|_2^2 \geq \left(2\text{real}(\bar{w}^T \hat{h}_k^T \hat{h}_k w) - \|\hat{h}_k \bar{w}\|_2^2 \right). \tag{25}$$

According to (19) and (25), the constraint condition (24b) can be transformed into a convex constraint as follows:

$$\left(2\text{real}(\bar{w}^T \hat{h}_k^T \hat{h}_k w) - \|\hat{h}_k \bar{w}\|_2^2 \right) p_k \geq \frac{t'_k{}^{(n)}}{2b_k{}^{(n)}} b_k'^2 + \frac{b_k'^{(n)}}{2t'_k{}^{(n)}} t_k'^2. \tag{26}$$

According to (9a) and (25), the constraint condition (10c) can be transformed into the following convex constraint.

$$\left(2\text{real}(\bar{w}^T \hat{h}_k^T \hat{h}_k w) - \|\hat{h}_k \bar{w}\|_2^2 \right) I_1 - I_2 \geq \left(2^{R_k^{min}} - 1 \right) \sigma_v^2, \tag{27}$$

where $I_1 = \left(p_k - \left(2^{R_k^{min}} - 1 \right) \sum_{j=1}^{k-1} p_j \right)$, $I_2 = \left(2^{R_k^{min}} - 1 \right) \sigma_u^2 / \beta_k$.

Similarly, the energy harvesting QoS constraint condition (10d) can be transformed into a convex constraint as:

$$\left(2\text{real}(\bar{w}^T \hat{h}_k^T \hat{h}_k w) - \|\hat{h}_k \bar{w}\|_2^2 \right) \sum_{j=1}^K p_j + \sigma_v^2 \geq \frac{P_k^{min}}{\eta(1 - \beta_k)}. \tag{28}$$

According to the feasible region of the continuous phase modulation network, the constraint condition (10g) can be transformed as follows:

$$|[w_i]| \leq \frac{1}{\sqrt{2}}. \tag{29}$$

As a result, problem (23) can be transformed into the following form.

$$\max_{w, b'_k, t'_k} \sum_{k=1}^K \log_2 (1 + t'_k) \tag{30a}$$

$$s. t. (10e), (24c), (26), (27), (28), (29) \quad (30b)$$

In problem (30), (10e) and (24c) are second-order conical convex constraints. (26), (27) and (28) are linear convex constraints. (29) is the first-order conic convex constraint. Therefore, problem (30) is a convex optimization problem, which can be solved directly by the convex optimization tool CVX. The specific algorithmic procedure is shown in Algorithm 2.

Algorithm 2: SCA-based simulated precoding iterative optimization algorithm

- 1) Parameter settings: fix the reflection matrix $\Phi^{(0)}$, initialize the auxiliary variables $\{t_k^{(0)}, b_k^{(0)}\}$ and analog precoding vector $\bar{w}^{(0)}$, the number of iterations $r = 1$, the maximum number of iterations is r_{max} ;
 - 2) for $r = 1: r_{max}$
 - 3) For the given $\{t_k^{(0)}, b_k^{(0)}\}$ and $\{\Phi^{(0)}\bar{w}^{(0)}\}$ solve according to Eq. (30) to obtain $t_k^{(r)}, b_k^{(r)}$ and $\bar{w}^{(r)}$
 - 4) Based on obtaining $t_k^{(r)}, b_k^{(r)}$ and $\bar{w}^{(r)}$ updating $t_k^{(0)}, b_k^{(0)}$ and $\bar{w}^{(r)}$
 - 5) If $t_k^{(r)}$ converges, jump out of the loop and output directly;
 - 6) Otherwise continue to iterate until the for loop ends
 - 7) Output: optimal objective values w^*
-

C. Optimization of Φ Under Fixed w, p_k and β_k

In this section, given the power allocation p_k , power splitting β_k and analog precoding vectors w , and then the IRS reflection matrix Φ is solved and optimized. The original question (10) is transformed to

$$\max_{\Phi} \sum_{k=1}^K \log_2 \left(1 + \frac{\|h_k \Phi G w\|_2^2 p_k}{\|h_k \Phi G w\|_2^2 \sum_{j=1}^{k-1} p_j + \sigma_v^2 + \frac{\sigma_u^2}{\beta_k}} \right) \quad (31a)$$

$$s. t. (10c), (10d), (10f) \quad (31b)$$

It is obvious that the problem (31) is non-convex and cannot be solved directly. We first relax the discrete θ to a continuous value of $[0, 2\pi]$, and set $\Omega = Gw, c_k = h_k \text{diag}(\Omega), \theta = [\lambda_1 e^{j\theta_1}, \dots, \lambda_{N_{IRS}} e^{j\theta_{N_{IRS}}}]^H$. Problem (31) can be transformed as follows:

$$\max_{\theta} \sum_{k=1}^K \log_2 \left(1 + \frac{\|c_k \theta\|_2^2 p_k}{\|c_k \theta\|_2^2 \sum_{j=1}^{k-1} p_j + \sigma_v^2 + \frac{\sigma_u^2}{\beta_k}} \right) \quad (32a)$$

$$s. t. (10c), (10d), (10f) \quad (32b)$$

It can be found that the objective functions of problem (32) and problem (23) have the same form, so problem (32) can be treated in the same way as problem (23). We introduce auxiliary variables t_k'' and b_k'' , and question (32) is transformed into the following form.

$$\max_{\theta} \sum_{k=1}^K \log_2(1 + t_k'') \tag{33a}$$

$$\text{s. t. (10c), (10d), (10f)} \tag{33b}$$

$$\|c_k \theta\|_2^2 p_k \geq \frac{t_k''^{(n)}}{2b_k''^{(n)}} b_k''^2 + \frac{b_k''^{(n)}}{2t_k''^{(n)}} t_k''^2 \tag{33c}$$

$$\|c_k \theta\|_2^2 \sum_{j=1}^{k-1} p_j + \sigma_v^2 + \frac{\sigma_u^2}{\beta_k} \leq b_k'' \tag{33d}$$

At this point, the method of solving the problem (24) is adopted to solve the problem (33). Similarly, we first use first-order Taylor expansion to simplify the non-convex problem, and the constraint condition (33b) can be transformed into

$$\left(2\text{real}\left(\bar{\theta}^T c_k^T c_k^T \theta\right) - \|c_k \theta\|_2^2\right) \geq \frac{t_k''^{(n)}}{2b_k''^{(n)}} b_k''^2 + \frac{b_k''^{(n)}}{2t_k''^{(n)}} t_k''^2. \tag{34}$$

According to equation (27), constraint condition (10c) can be simplified as follows:

$$\left(2\text{real}\left(\bar{\theta}^T c_k^T c_k^T \theta\right) - \|c_k \theta\|_2^2\right) I_1 - I_2 \geq \left(2^{R_k^{\min}} - 1\right) \sigma_v^2, \tag{35}$$

where $I_1 = \left(p_k - \left(2^{R_k^{\min}} - 1\right) \sum_{j=1}^{k-1} p_j\right)$, $I_2 = \left(2^{R_k^{\min}} - 1\right) \sigma_u^2 / \beta_k$.

Similarly, according to (28), the constraint condition (10d) can be simplified as

$$\left(2\text{real}\left(\bar{\theta}^T c_k^T c_k^T \theta\right) - \|c_k \theta\|_2^2\right) \sum_{j=1}^K p_j + \sigma_v^2 \geq \frac{P_k^{\min}}{\eta(1 - \beta_k)}. \tag{36}$$

Finally, question (33) can be translated as follows:

$$\max_{\theta, t_k'', b_k''} \sum_{k=1}^K \log_2(1 + t_k'') \tag{37a}$$

$$\text{s. t. (34), (35), (36), (10f), (33c)} \tag{37b}$$

It can be found that the constraints (34), (35), and (36) are linear constraints. (10f) is a first-order cone-convex constraint, and (33c) is a second-order cone-convex constraint. Therefore, problem (37) is a convex optimization problem, which can be solved using the existing convex optimization tool CVX.

In solving the reflection matrix Φ , the objective value obtained by problem (37) is the upper limit of the reflection matrix design problem (31) due to the relaxation. According to the solution of problem (37), the discrete phase shift value is

$$\vartheta_{N_j} = \arg \min_{\Omega} \left\{ \theta - \text{angle} \left(\theta_{N_j} \right) \right\}. \quad (38)$$

This discrete phase shift ϑ_{N_i} may not be a locally optimal solution due to quantization errors. However, as the IRS resolution B increases, the discrete phase shift IRS can achieve the performance of the algorithm. The continuous phase shift θ is optimized at each iteration. We update $\vartheta_{N_{IRS}}$ when the problem (37) converges.

Finally, we summarize the proposed alternative iterative optimization scheme in Algorithm 3. Based on the above derivations, the details of the proposed Joint Alternative Iterative Optimization algorithm are summarized in Algorithm 3.

Algorithm 3: proposed Joint Alternative Iterative Optimization Algorithm Base AO and SCA

- 1) Initialization: Feasible reflection matrix $\Phi^{(0)}$ and analog precoding vector $w^{(0)}$, auxiliary variables, iteration number $t = 1$, maximum iteration number t_{max} .
 - 2) Repeat:
 - 3) Initialize variables $t_k^{(0)}, b_k^{(0)}$, iteration number $r = 1$, maximum iteration number r_{max} .
 - 4) Repeat: Obtain $t_k^{(r)}, b_k^{(r)}, \beta_k^{(r)}$ and $p_k^{(r)}$ by solving (22).
Update variables $t_k^{(0)}, b_k^{(0)}$ according $t_k^{(r)}, b_k^{(r)}$.
Update $r = r + 1$.
 - 5) Until $r = r_{max}$ or Convergence;
 - 6) Initialize variables $t_k^{(0)}, b_k^{(0)}$, iteration number $r = 1$.
 - 7) Repeat: Obtain $t_k^{(r)}, b_k^{(r)}$ and $\bar{w}^{(r)}$ by solving (31).
Update variables $t_k^{(0)}, b_k^{(0)}$ and $\bar{w}^{(0)}$ according $t_k^{(r)}, b_k^{(r)}$ and $\bar{w}^{(r)}$.
Update $r = r + 1$.
 - 8) until $r = r_{max}$ or Convergence;
 - 9) Initialize variables $t_k^{(0)}, b_k^{(0)}$, iteration number $r = 1$.
 - 10) Repeat: Obtain $t_k^{(r)}, b_k^{(r)}$ and $\bar{\theta}^{(r)}$ by solving (37).
Update variables $t_k^{(0)}, b_k^{(0)}$ and $\bar{\theta}^{(0)}$ according $t_k^{(r)}, b_k^{(r)}$ and $\bar{\theta}^{(r)}$.
Update $r = r + 1$.
 - 11) Until $r = r_{max}$ or Convergence;
Update $\theta^{(*)}$. according to (38). Convert $\theta^{(*)}$ to Φ^* .
Update $t = t + 1$;
 - 12) Until $t = t_{max}$ or Convergence;
Obtain power allocation p_k^* , power splitting β_k^* , analog precoding w^* and reflection matrix Φ^* .
-

4. Numerical Results

In this section, we conduct a simulation analysis and verification of the performance of the proposed scheme. Specifically, the BS is equipped with an ULA of $N_{TX} = 64$ antennas and $N_{RF}=1$ to serve $K = 4$ users, the parameters are set as $F = 3$, including one line of sight (LoS) component and two non-line-of-sight (NLoS) components; We set Number of RIS reflection elements $N_{IRS} = 10$, $\eta = 0.9$, the user's minimum collection energy and user service quality are $P_k^{min} = 0.1\text{mW}$ and $R_k^{min} = 0.1\text{bit/s /Hz}$

Fig. 3 illustrates the effect of IRS resolution on the spectral efficiency of the system. From **Fig. 3**, it can be seen that the difference in system spectral efficiency between the continuous and discrete phase shifts decreases as the quantization bit B increases, which is due to the fact that a larger B increases the degree of freedom of the IRS, which allows for better regulation of the IRS phase shift.

Fig. 4 demonstrates the system spectral efficiency versus the total system transmit power for different schemes, where the quantization bit B is set to 4. It can be seen that the spectral efficiency of all schemes increases with the increase of the total transmit power. Moreover, it can be found that the spectral efficiency of the proposed system based on continuous phase modulation network is superior to that based on conventional phase shifter modulation network. Further, the proposed scheme is superior to the OMA scheme because all the NOMA users can be served simultaneously compared to the OMA system.

Fig. 5 illustrates the relationship between the spectral efficiency of the system and the number of IRS reflective elements for different schemes, where $B = 4$ and $P_{max} = 5\text{dB}$. It can be seen that the spectral efficiency increases with the number of reflective elements for all schemes. This is due to the fact that the more IRS passive elements, the higher the reflected signal power and the higher the power gain. Moreover, the proposed scheme is also superior to the conventional phase shifter-based modulation network, which is consistent with **Fig. 4**. Similarly, the spectral efficiency of the NOMA scheme is also superior to the OMA scheme.

Fig. 6 illustrates the relationship between the spectral efficiency of the system and the number of IRS reflective elements for different schemes. It can be seen that the spectral efficiency of all schemes increases with the number of antennas, but its growth rate gradually slows down. From **Fig. 5** and **Fig. 6**, it is found that increasing the number of IRS reflective elements and the number of transmitting antennas at the base station increases the system spectral efficiency. This is due to the fact that when there are more antennas at the base station or more reflective elements at the IRS, a higher beamforming gain can be achieved.

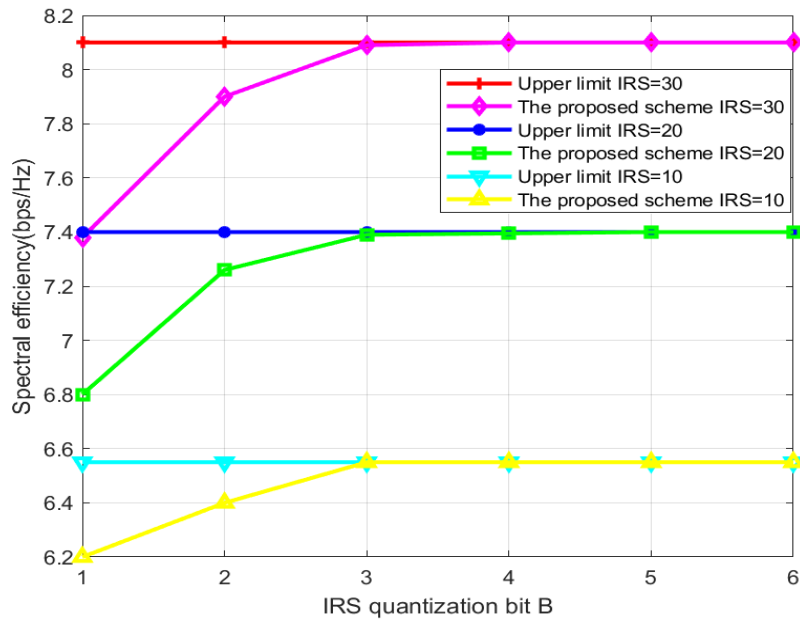


Fig. 3. The relationship between system spectral efficiency and IRS quantization bit B

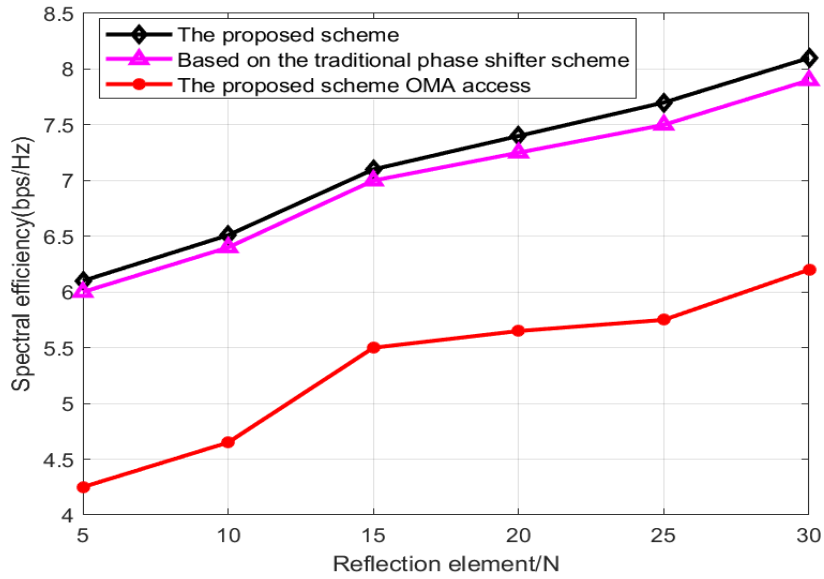


Fig. 4. The relationship between system spectrum efficiency and the number of IRS reflection elements.

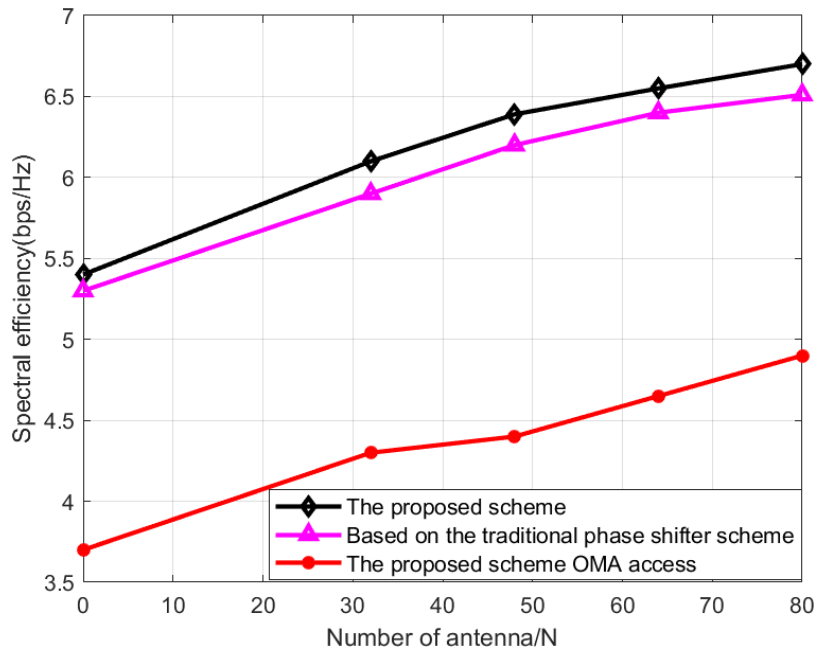


Fig. 5. The relationship between the spectral efficiency of the system and the number of antennas.

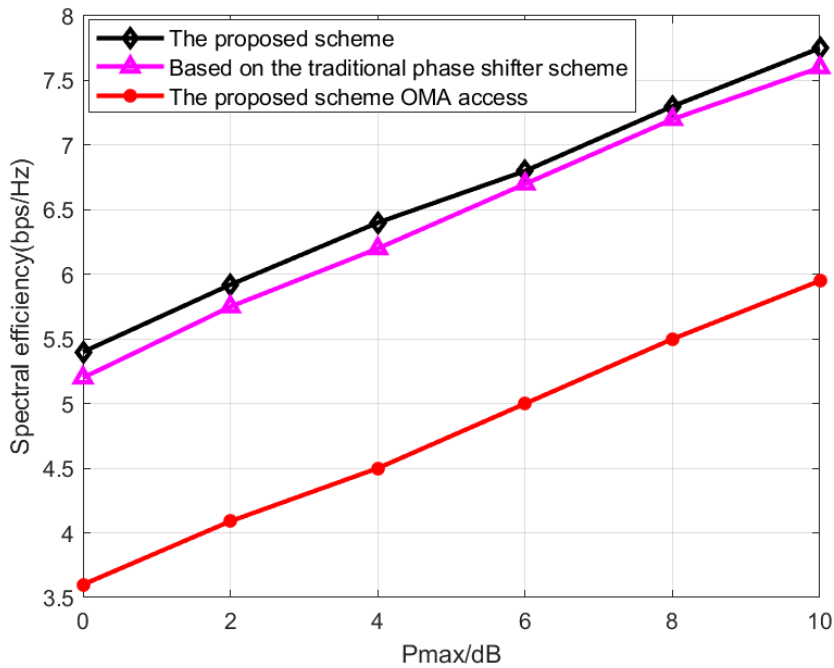


Fig. 6. The relationship between the spectral efficiency of the system under different scenarios and P_{max}

5. Conculsions

In this paper, the spectrum efficiency in the IRS-assisted mMIMO-NOMA system is studied to realize the optimal resource allocation. The sparse RF chain antenna structure with continuous phase modulation is introduced to reduce the energy consumption. The joint optimization strategy for power allocation, power splitting factor, analog precoding vector and

IRS reflection matrix is proposed to maximize spectral efficiency under the constraints of user service quality, minimum energy collection and total transmitted power. On this basis, the above non-convex optimization problem is solved by the proposed three-stage joint optimization algorithm. The simulation results show that IRS can effectively improve the spectral efficiency of the system and the spectral efficiency of the NOMA transmission scheme is higher than that of the traditional scheme. The algorithm proposed in this paper not only realize the maximization spectral efficiency, but also provide strong theoretical support and practical guidance for the future-oriented communication. However, there are still directions for further research in the future. For example, future research can further explore the impact of the IRS element and the distance between different equipment on the fairness of users and the system performance. In addition, the resource allocation optimization problem in the non-ideal system condition should be further studied.

Acknowledgements

The work was supported by the National Natural Science Foundation of China under Grant 62101613 and Henan science and technology planning project under Grant 222102210068.

We thank the anonymous referees for their helpful comments and suggestions on the initial version of this paper.

References

- [1] W. Huang and Z. Ding, "New Insight for Multi-User Hybrid NOMA Offloading Strategies in MEC Networks," *IEEE Transactions on Vehicular Technology*, vol.73, no.2, pp.2918-2923, Feb. 2024. [Article\(CrossRefLink\)](#)
- [2] S. Elhoushy, M. Ibrahim and W. Hamouda, "Downlink Performance of CF Massive MIMO Under Wireless-Based Fronthaul Network," *IEEE Transactions on Communications*, vol.71, no.5, pp.2632-2653, May 2023. [Article\(CrossRefLink\)](#)
- [3] I. Khaled, C. Langlais, A. E. Falou, B. A. Elhassan and M. Jezequel, "Multi-User Angle-Domain MIMO-NOMA System for mmWave Communications," *IEEE Access*, vol.9, pp.129443-129459, 2021. [Article\(CrossRefLink\)](#)
- [4] P. Jain and A. Gupta, "Performance Analysis of Massive MIMO Millimeter Wave NOMA HetNet," in *Proc. of 2022 International Conference on Emerging Smart Computing and Informatics (ESCI)*, pp.1-5, 2022. [Article\(CrossRefLink\)](#)
- [5] A. A. Saleh and M. A. Ahmed, "Multiuser Beamforming System with Massive MIMO-NOMA over mmWave Channel," in *Proc. of 2023 1st International Conference on Advanced Engineering and Technologies (ICONNIC)*, pp.269-274, 2023. [Article\(CrossRefLink\)](#)
- [6] L. Pang et al., "Joint Power Allocation and Hybrid Beamforming for Downlink mmWave-NOMA Systems," *IEEE Transactions on Vehicular Technology*, vol.70, no.10, pp.10173-10184, Oct. 2021. [Article\(CrossRefLink\)](#)
- [7] X. Qi, X. Gang and Y. Liu, "Hardware-Efficient Hybrid Precoding and Power Allocation in Multi-User mmWave-NOMA Systems," in *Proc. of 2020 IEEE/CIC International Conference on Communications in China (ICCC)*, pp.184-189, 2020. [Article\(CrossRefLink\)](#)
- [8] X. Qi, G. Xie and Y. Liu, "Energy-Efficient Power Allocation in Multi-User mmWave-NOMA Systems With Finite Resolution Analog Precoding," *IEEE Transactions on Vehicular Technology*, vol.71, no.4, pp.3750-3759, Apr. 2022. [Article\(CrossRefLink\)](#)
- [9] A. Jee and S. Prakriya, "Performance of Energy and Spectrally Efficient AF Relay-Aided Incremental CDRT NOMA-Based IoT Network With Imperfect SIC for Smart Cities," *IEEE Internet of Things Journal*, vol.10, no.21, pp.18766-18781, Nov. 2023. [Article\(CrossRefLink\)](#)

- [10] A. Jee, K. Agrawal and S. Prakriya, "A Coordinated Direct AF/DF Relay-Aided NOMA Framework for Low Outage," *IEEE Transactions on Communications*, vol.70, no.3, pp.1559-1579, Mar. 2022. [Article\(CrossRefLink\)](#)
- [11] A. Jee and S. Prakriya, "Novel Channel Aware Power Control for a Multi-User Downlink NOMA Network," *IEEE Wireless Communications Letters*, vol.13, no.2, pp.392-396, Feb. 2024. [Article\(CrossRefLink\)](#)
- [12] Y. Hei, S. Yu, C. Liu, W. Li and J. Yang, "Energy-Efficient Hybrid Precoding for mmWave MIMO Systems With Phase Modulation Array," *IEEE Transactions on Green Communications and Networking*, vol.4, no.3, pp.678-688, Sep. 2020. [Article\(CrossRefLink\)](#)
- [13] X. Yu, F. Xu, K. Yu, and X. Dang, "Power Allocation for Energy Efficiency Optimization in Multi-User mmWave-NOMA System With Hybrid Precoding," *IEEE Access*, vol.7, pp.109083-109093, 2019. [Article\(CrossRefLink\)](#)
- [14] L. Zhu, J. Zhang, Z. Xiao, X. Cao, D. O. Wu, and X. -G. Xia, "Millimeter-Wave NOMA With User Grouping, Power Allocation and Hybrid Beamforming," *IEEE Transactions on Wireless Communications*, vol.18, no.11, pp.5065-5079, Nov. 2019. [Article\(CrossRefLink\)](#)
- [15] K. Zhang, C. Liu, H. Wang and Y. Song, "An IRS-Aided mmWave Massive MIMO Systems Based on Genetic Algorithm," in *Proc. of 2020 IEEE 20th International Conference on Communication Technology (ICCT)*, pp.288-293, 2020. [Article\(CrossRefLink\)](#)
- [16] X. Qi, X. Gang and Y. Liu, "Hardware-Efficient Hybrid Precoding and Power Allocation in Multi-User mmWave-NOMA Systems," in *Proc. of 2020 IEEE/CIC International Conference on Communications in China (ICCC)*, pp.184-189, 2020. [Article\(CrossRefLink\)](#)
- [17] F. Zhao, W. Hao, L. Shen, G. Sun, Y. Zhou and Y. Wang, "Secure Energy Efficiency Transmission for mmWave-NOMA System," *IEEE Systems Journal*, vol.15, no.2, pp.2226-2229, Jun. 2021. [Article\(CrossRefLink\)](#)
- [18] J. Bai, "Adaptive Optimization Scheme for RIS-Aided mmWave-NOMA Systems with Hybrid Beamforming," in *Proc. of 2023 3rd International Conference on Communication Technology and Information Technology (ICCTIT)*, pp.55-58, 2023. [Article\(CrossRefLink\)](#)
- [19] M. Zeng, W. Hao, O. A. Dobre and H. V. Poor, "Energy-Efficient Power Allocation in Uplink mmWave Massive MIMO With NOMA," *IEEE Transactions on Vehicular Technology*, vol.68, no.3, pp.3000-3004, Mar. 2019. [Article\(CrossRefLink\)](#)
- [20] D. Galappaththige and C. Tellambura, "Sum Rate Maximization for RSMA-Assisted CF mMIMO Networks With SWIPT Users," *IEEE Wireless Communications Letters*, vol.13, no.5, pp.1300-1304, May 2024. [Article\(CrossRefLink\)](#)
- [21] L. Zhu, J. Zhang, Z. Xiao, X. Cao, D. O. Wu and X. -G. Xia, "Millimeter-Wave NOMA With User Grouping, Power Allocation and Hybrid Beamforming," *IEEE Transactions on Wireless Communications*, vol.18, no.11, pp.5065-5079, Nov. 2019. [Article\(CrossRefLink\)](#)
- [22] C. Sun, S. Yang, Y. Chen, J. Guo and Z. Nie, "An Improved Phase Modulation Technique Based on Four-Dimensional Arrays," *IEEE Antennas and Wireless Propagation Letters*, vol.16, pp.1175-1178, 2017. [Article\(CrossRefLink\)](#)
- [23] Y. Hei, S. Yu, C. Liu, W. Li and J. Yang, "Energy-Efficient Hybrid Precoding for mmWave MIMO Systems With Phase Modulation Array," *IEEE Transactions on Green Communications and Networking*, vol.4, no.3, pp.678-688, Sep. 2020. [Article\(CrossRefLink\)](#)
- [24] Y. Xiu et al., "Reconfigurable Intelligent Surfaces Aided mmWave NOMA: Joint Power Allocation, Phase Shifts, and Hybrid Beamforming Optimization," *IEEE Transactions on Wireless Communications*, vol.20, no.12, pp.8393-8409, Dec. 2021. [Article\(CrossRefLink\)](#)
- [25] V. Jamali, A. M. Tulino, G. Fischer, R. R. Müller and R. Schober, "Intelligent Surface-Aided Transmitter Architectures for Millimeter-Wave Ultra Massive MIMO Systems," *IEEE Open Journal of the Communications Society*, vol.2, pp.144-167, 2021. [Article\(CrossRefLink\)](#)
- [26] P. Wang, J. Fang, X. Yuan, Z. Chen and H. Li, "Intelligent Reflecting Surface-Assisted Millimeter Wave Communications: Joint Active and Passive Precoding Design," *IEEE Transactions on Vehicular Technology*, vol.69, no.12, pp.14960-14973, Dec. 2020. [Article\(CrossRefLink\)](#)

- [27] Y. Zhang et al., "Performance Analysis of CF-mMIMO-Aided SWIPT IoT Networks With Nonideal RF Response and Low-Resolution ADCs/DACs," *IEEE Sensors Journal*, vol.24, no.3, pp.3594-3607, Feb. 2024. [Article\(CrossRefLink\)](#)
- [28] J. Tang et al., "Joint Power Allocation and Splitting Control for SWIPT-Enabled NOMA Systems," *IEEE Transactions on Wireless Communications*, vol.19, no.1, pp.120-133, Jan. 2020. [Article\(CrossRefLink\)](#)
- [29] L. Dai, B. Wang, M. Peng and S. Chen, "Hybrid Precoding-Based Millimeter-Wave Massive MIMO-NOMA With Simultaneous Wireless Information and Power Transfer," *IEEE Journal on Selected Areas in Communications*, vol.37, no.1, pp.131-141, Jan. 2019. [Article\(CrossRefLink\)](#)
- [30] S. Kumar, A. Jee and S. Prakriya, "Performance Analysis and Optimization of Partitioned-IRS-Assisted NOMA Network," *IEEE Wireless Communications Letters*, vol.13, no.3, pp.761-765, Mar. 2024. [Article\(CrossRefLink\)](#)



Bing Ning received the Ph. D. degree from information and communication engineering with Zhengzhou University, Zhengzhou, China, in 2016. Now, she is an Associate Professor at the School of Information and Communication Engineering, Zhongyuan University of Technology, China. Her research interests are in the areas of wireless communications, including cognitive radio, backscatter communication, and wireless body area network.



Li Shuang is currently enrolled in the Electronic Information major, School of Information and Communication Engineering at Zhongyuan University of Technology. Her research interests are in the field of wireless communication, including backscatter communication and wireless body area networks.



Wu Xinli graduated from School of Information Engineering, majoring in Electronic and Communication Engineering, Zhengzhou University. His research interests include millimeter wave communication, NOMA wireless communication, and resource allocation.



Hao Wanming received the Ph. D. degree from School of Electrical and Electronic Engineering, Kyushu University, Japan, in 2018. He worked as a Research Fellow at the 5G Innovation Center, Institute of Communication Systems, University of Surrey, U.K. Now, he is an Associate Professor at the School of Electrical and Information Engineering, Zhengzhou University, China. His research interests include millimeter wave and RIS. He is the editor of IEEE O-JCS.